



## Does environmental risk really change in abandoned mining areas in the medium term when no control measures are taken?

Luis Rodríguez<sup>a,\*</sup>, Beatriz González-Corrochano<sup>b</sup>, Hassay L. Medina-Díaz<sup>a</sup>,  
Francisco J. López-Bellido<sup>a</sup>, Francisco J. Fernández-Morales<sup>a</sup>, Jacinto Alonso-Azcárate<sup>b</sup>

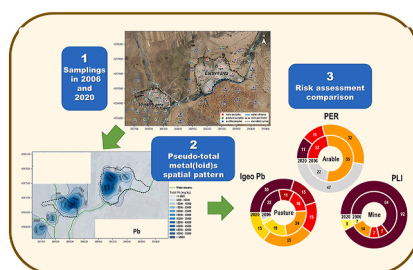
<sup>a</sup> Chemical Engineering Department, Institute for Chemical and Environmental Technology ITQUIMA, University of Castilla-La Mancha, Avenida Camilo José Cela, S/n, 13071, Ciudad Real, Spain

<sup>b</sup> Department of Physical Chemistry, Faculty of Environmental Sciences and Biochemistry, University of Castilla-La Mancha, Avenida Carlos III, S/n, 45071, Toledo, Spain

### HIGHLIGHTS

- Mine tailings, arable land and pastureland samples were taken and analyzed.
- Environmental risk was assessed by using several pollution risk indices.
- Environmental hazard was mainly due to high levels of Pb and Zn.
- Metals in pastureland plots were one order of magnitude higher than background values.
- Metal (loid)s dispersion really increased the environmental risk in the studied period.

### GRAPHICAL ABSTRACT



### ARTICLE INFO

Handling Editor: X. Cao

#### Keywords:

Polluted soils  
Pb/zn mines  
Environmental risk assessment  
Pollution load index  
Geoaccumulation index  
Potential ecological risk index

### ABSTRACT

Studies regarding how environmental risk evolves in abandoned mining areas in the medium term have been seldom carried out. The answer to this question is not obvious despite it is essential in order to evaluate the need to take urgent control measures in these areas. Fifty-two samples corresponding to soils (from natural pasture and arable lands) and mine tailings were collected in the surroundings of an old Spanish Pb/Zn mine (San Quintín, Central Spain). Current concentrations of pseudo-total and available metal (loid)s (Pb, Zn, Cd, Cu, As and Ag) were determined and the environmental risk assessment (ERA) was conducted with these data and those corresponding to a sampling previously carried out in 2006. ERA was carried out by calculating the geoaccumulation index (Igeo), the pollution load index (PLI) and the potential ecological risk index (PER). Results demonstrated that Pb and Zn concentrations have increased in the soils of the plots surrounding the mining areas causing a moderate rise in most of the determined pollution indices between 2006 and 2020. It was especially significant in the pastureland areas, with increases up to 17% in the number of soil samples that reached the highest risk classification in 2020 as compared to those taken in 2006. The results obtained here demonstrate that the environmental risk can actually increase in a continuous way in abandoned mining areas despite the closure of the mining operation and the effect of the possible natural attenuation.

\* Corresponding author.

E-mail address: [luis.rromero@uclm.es](mailto:luis.rromero@uclm.es) (L. Rodríguez).

## 1. Introduction

Environmental hazard derived from abandoned metal mines throughout the world has been highlighted in previous studies on soil pollution, especially those arising from lead-zinc ores (Bhattacharya et al., 2006; Chopin et al., 2003; Gitari et al., 2018; Liu et al., 2019). The presence in these areas of tailings, ponds, dumps, and other type of wastes without any measure of environmental control causes over time and with the participation of the climatic agents, such as rain and wind, the pollution of soils (Asare and Afriyie, 2021), water (Concas et al., 2006), air (Djebbi et al., 2017) and biota (Bănăduc et al., 2021). The remoteness and the extension of these areas, together with the extinction of the mining companies responsible for the contamination, makes the environmental recovery costly and difficult; as a result, there are numerous mining areas that remain polluting many years after their closure.

One of the most used and easiest ways to assess the environmental risk in soils is the calculation of some pollution indices based on the comparison of the actual metal concentrations in soil samples and the background levels of those metals in the study area. The geoaccumulation index (Igeo) was firstly introduced to study basal sediments but, up to the present, it has been widely used to characterize anthropogenic pollution in soils (Doabi et al., 2018; Tian et al., 2018; Zhou et al., 2020). The pollution load index (PLI) is a composite index (Tomlinson et al., 1980) that allows to estimate the environmental risk associated to several metals in multi-contaminated soils such as existing in metal mining areas; it is calculated from the individual pollution indices of each considered metal (Chen et al., 2015; Fernández-Caliani et al., 2009; Qing et al., 2015). Other pollution indices are not only based on the increase of metal contents with respect to the background ones but also consider the toxicity of metals and the response of the environment; the potential ecological risk index (PER) was proposed by Hakanson (1980) to quantitatively evaluate the pollution of sediments by metals, but it has been also used to assess metal contamination and ecological hazards in soils (Islam et al., 2015; Liu et al., 2020; Luo et al., 2007; Rehman et al., 2018; Zhou et al., 2020).

Studies on risk assessment in abandoned mining areas are relatively numerous in the scientific literature. However, there are at least two aspects that have not been enough addressed to date. On one hand, most of the studies have been focused on the characterization of metal concentrations and risk assessment in waste dump areas and others belonging to mining facilities, while far few works have carried out a systematic characterization of the surrounding agricultural and livestock areas (Fernández-Caliani et al., 2009; López et al., 2008; Tian et al., 2018). On the other hand, practically all of the previous papers analyze the contamination and/or the associated hazard in these mining sites at a given time, while it is difficult to find studies that include samplings carried out over a long period of time (Aguilar et al., 2004; Kicińska, 2019, 2020). This last aspect seems very important to us because it would allow to have relevant information about the evolution of environmental risk when control measures are not implemented. Moreover, it is not evident that environmental risk increases indefinitely in abandoned mining areas that were closed a long time ago since the natural attenuation processes (e.g. those carried out by plants and other geochemical and edaphic ones) could lead to the immobilization of pollutants to some extent. In fact, Kicińska (Kicińska, 2019, 2020) reported an increase of non soluble and residual soil metal fractions after 20 years in a study conducted in the close vicinity of a zinc-works area located in Poland.

Considering the above and given that our research team had the characterization data from a sampling carried out in 2006 in the San Quintín mine area (Rodríguez et al., 2009), we planned to carry out a new sampling in this area with two objectives: (i) the characterization of the current contamination by metal (loid)s and the associated environmental risk both in the area covered with mining waste and in the surrounding agricultural and livestock areas, and (ii) compare the current

environmental risk with that existing in the previous sampling carried out 14 years earlier. To achieve those goals, a new sampling was carried out in 2020 using the same methodology used in the previous one, and the values of several risk assessment indices widely used in the literature have been calculated in order to carry out the comparative study of the evolution of pollution in the studied area.

## 2. Materials and methods

### 2.1. Studied area

San Quintín mining area is located in the Alcudia Valley mining district, Ciudad Real (Spain), approximately 250 km south Madrid. It was an important producer of Pb, Zn and Ag in the late nineteenth and early twentieth centuries, being galena (PbS) and sphalerite (ZnS) the main ore minerals. A more detailed description of the history of this mining group has been reported elsewhere (García-Lorenzo et al., 2019; Rodríguez et al., 2009). Currently, it consists of two different mine sectors, i.e. Eastern and Western (Fig. 1), with approximate areas of 460,000 and 160,000 m<sup>2</sup>, respectively, covered by rock waste, tailings and old buildings corresponding to different phases of mining exploitation (Sánchez-Donoso et al., 2019). The sampled area also includes the plots that surround the mining areas, dedicated to crops such as olive trees, barley or oat and cattle farming. This area has a continental Mediterranean climate characterized by very marked differences in temperature and rainfall between summer and winter; the annual rainfall is about 400 mm, and the average annual temperature is around 16 °C (Sánchez-Donoso et al., 2019).

### 2.2. Sampling

The sampling of the studied area was carried out in the same way to that accomplished in 2006 (Rodríguez et al., 2009). Soil samples were taken from 0 to 20 cm depth using a systematic random sampling based on two grids centered in each of the two sectors of San Quintín mine (Fig. 1). The grid corresponding to the East sector was composed of 30 rectangular cells of 300 m length and 230 m height; thirty samples were taken in this sector. The grid for the sampling of the West sector was initially designed with 30 rectangular cells of 220 m length and 210 m height; however, the impossibility of access to a fenced area of private property meant that we could only take 22 samples of the 30 initially planned. On the overall, 52 samples were taken (Fig. 1); twenty corresponded to plots dedicated to agricultural crops (arable land samples); nineteen to cattle grazing areas (pastureland samples) and thirteen to mining areas (mine tailings samples). Samples were put and labelled in polyethylene bags for their transport to the laboratory. Once there, the samples were manually disaggregated and allowed to dry at approximately 25 °C during 72 h; finally, they were sieved to 2 mm and stored at 4 °C prior to their analysis.

### 2.3. Sample characterization

Chemical characterization of the samples included the analysis of the following parameters: pH (in water), electrical conductivity (EC), total and organic carbon and the concentration of pseudo-total and CaCl<sub>2</sub>-extractable Pb, Zn, Cd, Cu, As and Ag. Milli-Q water and Hiperpur quality reagents were used for all the analysis and the results were referred to dry weight (water content of the samples was determined by heating in an oven at 105 °C to constant weight).

Sample pH was measured in a 1:5 soil-water (w:v) mixture using the ISO 10390-2005 method. EC was measured in a 1:5 soil-water (w:v) using a conductometer. Total organic and inorganic carbon were analyzed using a TOC analyzer (Shimadzu TOC-VCSH, Columbia, USA); organic carbon was calculated by subtracting both parameters. Pseudo-total and CaCl<sub>2</sub>-extractable metal (loid) concentrations were analyzed in the digested/extracted samples by means of ICP-MS using a Thermo

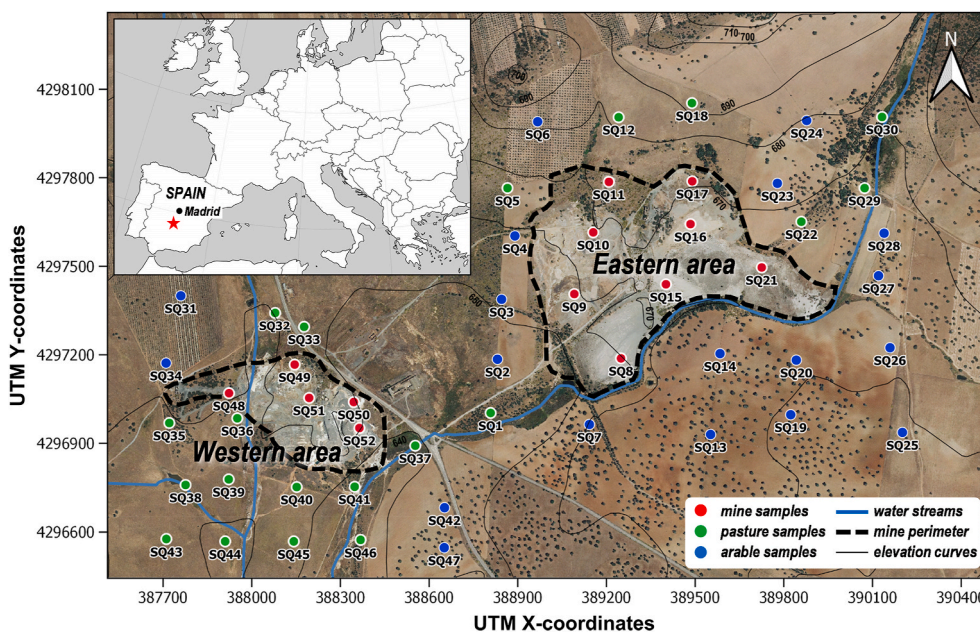


Fig. 1. Location map of the studied area and the sampling points corresponding to 2020, indicating the soil use type of the samples.

iCAP TQ spectrometer (ThermoFisher Scientific, Waltham, MA USA); all the samples were analyzed in triplicate. Prior to the analysis of pseudo-total metal (loid) concentrations, samples were digested in a microwave oven (CEM MARS 5, Matthews, USA) using the EPA 3051 A method (0.5 g of soil sample were digested with a mixture of 9 mL of 69% w:w nitric acid and 3 mL of 37% w:w hydrochloric acid). Single extraction of the samples with  $\text{CaCl}_2$  was carried out by means of a procedure based on the method reported by Novozamsky et al. (1993); basically, 2 g of dry soil were extracted during 3 h with 20 mL of an aqueous solution of 0.01 M  $\text{CaCl}_2$ . SRM 2711 (Montana Soil, National Institute of Standards & Technology, USA) and BCR-483 (Sewage sludge amended soil, Community Bureau of Reference, Brussels, Belgium) certified reference materials were used to assess the accuracy of the pseudo-total and  $\text{CaCl}_2$ -extractable metal (loid) analysis, respectively; agreement between concentrations determined by us and those certified was in the range 88–100% for pseudo-total metal (loid)s and 100–129% for the extractable ones.

Mineralogical analysis of mine tailings and selected soil samples were carried out by X-ray diffraction (XRD) using a PANalytical® diffractometer, X'Pert Pro model, equipped with an X'celerator detector, using  $\text{CuK}\alpha$  radiation, a 45 Kv accelerating voltage and a 40 mA current. Bulk mineralogy was determined by the polycrystalline disoriented powder method after sample grinding and homogenizing in an automatic agate mortar and sieving to <0.053 mm. Semi-quantitative analysis of the obtained diffractograms was conducted by the Schultz's method.

#### 2.4. Environmental risk assessment

Environmental risk in San Quintín mine area was assessed by using three different pollution indices previously described in the literature; only Pb, Zn, Cd and Cu concentrations were considered since they were the only metals analyzed in the sampling carried out in 2006.

The geoaccumulation index (Igeo) was calculated by the original equation by Müller (Müller, 1969):

$$I_{geo} = \log_2 \left( \frac{C_i}{1.5B_i} \right) \quad (1)$$

being  $C_i$  the total concentration of the metal  $i$  in the sample and  $B_i$  the background concentration of this metal in the region where San Quintín

mine is located (Castilla-La Mancha, Spain). Those regional background values have been previously reported by Ballesta et al. (2010) and Bravo et al. (2019). Based on the values obtained for Igeo, samples can be classified as (Qing et al., 2015): <0, practically unpolluted; 0–1, unpolluted to moderately polluted; 1–2, moderately polluted; 2–3, moderately to strongly polluted; 3–4, strongly polluted; 4–5, strongly to extremely polluted; and >5, extremely polluted.

The Pollution Load Index (PLI) was calculated from the individual values of the Pollution Index (PI) for Pb, Zn, Cd and Cu according to Eq. (2) (Qing et al., 2015). The pollution index (also called concentration factor) is defined as the ratio between the total metal concentration in the sample and the corresponding regional background concentration (Fernández-Caliani et al., 2009; Qing et al., 2015).

$$PLI = (PI_{Pb} \cdot PI_{Zn} \cdot PI_{Cd} \cdot PI_{Cu})^{\frac{1}{4}} \quad (2)$$

According to PLI, samples were classified as follows (Chen et al., 2015):  $\leq 1$ , unpolluted; 1–2, unpolluted to moderately polluted; 2–3, moderately polluted; 3–4, moderately to highly polluted; 4–5, highly polluted; and >5, very highly polluted.

The Potential Ecological Risk index (PER) was calculated from the Eqs. (3) and (4).  $E_r^i$  is the potential ecological risk index for a single metal; it is a function of the pollution index and a 'toxic-response' factor ( $T_r^i$ ) of biological systems in soils and sediments. It has been used the  $T_r^i$  values proposed by Hakanson (1980), i.e. 5, 1, 30 and 5 for Pb, Zn, Cd and Cu, respectively; those values were calculated taking into account different factors, such as the abundance and historical accumulation of each metal in soils and sediments, along with the specific sensitivity of the ecosystems to them (Hakanson, 1980). The composite potential ecological risk index (PER) can be obtained as the sum of the individual ecological risk indices for each metal (Eq. (4)).

$$E_r^i = T_r^i \cdot PI_i \quad (3)$$

$$PER = \sum_1^n E_r^i \quad (4)$$

The ranges of PER values originally established by Hakanson for the risk classification were based in eight pollutants, i.e. PCBs, Hg, Cd, As, Cu, Pb, Cr and Zn (Hakanson, 1980). In our case, only four metals have been used (Pb, Zn, Cd and Cu), so an adjust of the original ranges must be carried out; it has been done with the method reported by Chen et al.



(2020). The sum of the  $T_r^i$  factors for the eight pollutants used by Hakanson was 133 while in this study it was only 41. Hakanson adopted the limiting value of 150 for the 'low risk' grade and established three additional ranges in multiples of this initial value (i.e. 150-300 for moderate risk, 300-600 for considerable risk and >600 for very high risk). In our case, the limiting value for low risk was obtained as follows:  $PER = 150 \times (41/133) = 46$ , that was adjusted to 50. So, the following ranges were used for the risk assessment classification based in the PER values calculated by us:  $PER > 50$ , low risk;  $50 \leq PER < 100$ , moderate risk;  $100 \leq PER < 200$ , considerable risk and  $PER \geq 200$ , very high risk.

Igeo, PLI and PER values corresponding to the samples taken in 2020 were obtained from the pseudo-total metal concentrations in the soil fraction <2 mm. Since the pseudo-total metal concentrations of the samples taken in 2006 (Rodríguez et al., 2009) corresponded to the <0.063 mm soil fraction, prior to the calculation of the pollution indices, those values have been referred to the <2 mm soil fraction by using the particle size distribution curves of each sample (data obtained in 2006 by laser diffraction). The ranges and the mean values of the recalculated metal concentrations for the samples taken in 2006 are shown in the Table S1 included in the Supplementary Material.

### 2.5. Statistical analysis

Statistical analysis of the results has been performed by using the software SPSS Statistic 24.0 (IBM, New York, USA). Differences in the mean values of pseudo-total metal (loid) concentrations and pollution indices for the three different types of soil samples was checked by means of ANOVA analysis using the Duncan test ( $p < 0.05$ ); log-transformed values of the variables were used when normality criteria were not reached (checked by the Kolmogorov-Smirnov test). Correlation between the concentrations of the different metal (loid)s was assessed by the Spearman's correlation coefficient. Matrix cluster analysis of metal (loid) concentrations was conducted by the Ward's method using Euclidean distance squared. Spatial distribution of Pb and Zn soil concentration was obtained by interpolation using the QGIS free open-source software (v 3.10).

## 3. Results and discussion

### 3.1. Current situation: metal(loid) distribution in San Quintín area

Table 1 shows the range and mean values for pseudo-total concentrations of Pb, Zn, Cd, Cu, As and Ag along with the percentage of  $CaCl_2$ -

extractable metal (loid)s found in the analyzed samples; they are grouped in three different soil uses, i.e. arable land, pastureland and mine tailings. As expected, considering the minerals exploited in the studied mining area, the most abundant metal (loid)s for all the sample types were Pb and Zn, with higher concentrations for Pb. Regarding the other metal (loid)s analyzed, the order of abundance was  $Cu > Ag > As > Cd$ . The high correlation found between the different metal (loid)s (Table 2) points out the common origin of most metal (loid) content in the soil samples, both in mine tailings and agro-livestock ones; it would show a first insight into the environmental hazard associated to the untreated mine waste located in the studied area. Electrical conductivity (EC) was also positively correlated with metal (loid) concentrations in a very statistically significant way ( $p < 0.01$ , Table 2). Since pH was poorly correlated with the pseudo-total metal (loid) contents (Table 2), the mentioned correlation with EC is indicative of the significant contribution of mobile ionic metal species to the overall EC of the soils (García-Carmona et al., 2019). However, concentrations of  $CaCl_2$ -extractable metals, i.e. exchangeable metals, were only significantly high for Zn and Cd (reaching up to 63 and 100% of the pseudo-total metal concentration, respectively); on the contrary, exchangeable Pb, Cu, As and Ag presented a very low proportion in all the samples (<1%), indicating low availability of these metal (loid)s.

Results can be more adequately discussed considering the different soil uses corresponding to the samples taken in the studied area. As a general trend, concentrations of all analyzed metal (loid)s were in the order mine tailings  $\gg$  pastureland  $>$  arable land. Previous works have shown that background regional concentrations of the studied metal (loid)s are 17.9, 35.0, 3.9, 10.9, 6.5 and 4.3  $mg\ kg^{-1}$  for Pb, Zn, Cd, Cu, As and Ag, respectively (Ballesta et al., 2010; Bravo et al., 2019). As expected, mean metal (loid) concentrations of mine tailings samples widely exceed the background values for all the metal (loid)s, with mean values that were 715 and 107 times their background ones for Pb and Zn, respectively, and one order of magnitude higher for the rest of metal (loid)s (Table 1). Samples taken in the pastureland plots adjacent to the mining waste areas also showed mean metal (loid) concentrations much higher than background values, in at least one order of magnitude (except for Cd), indicating spreading of pollution from the mining areas in some extent. Mean values of arable land samples were higher, in approximately one order of magnitude, than background concentrations for Pb and Zn, while the mean concentrations of the rest of metal (loid)s were similar or lower than background ones (Table 1). In a first view, it is evident that lead and zinc are responsible of most of the environmental hazard associated to the studied mining site which strongly

**Table 1**

Selected physicochemical properties, pseudo-total (p-total) metal concentrations and percentage of  $CaCl_2$ -extractable metals of soil samples taken from the San Quintín mine area in 2020 (different letters mean significant differences between sample types for each parameter, Duncan's test  $p < 0.05$ ).

| Sample type<br>Parameters          | Arable land (n = 20) |            | Pastureland (n = 19)  |            | Mine tailings (n = 13) |             |
|------------------------------------|----------------------|------------|-----------------------|------------|------------------------|-------------|
|                                    | Mean $\pm$ STD       | Range      | Mean $\pm$ STD        | Range      | Mean $\pm$ STD         | Range       |
| pH-H <sub>2</sub> O                | 6.08 $\pm$ 0.48a     | 5.17–6.87  | 6.45 $\pm$ 0.59a      | 5.18–7.29  | 5.21 $\pm$ 1.21 b      | 3.12–7.15   |
| EC ( $\mu S\ cm^{-1}$ )            | 66.7 $\pm$ 30.1 b    | 30.3–127.7 | 102.6 $\pm$ 94.4 b    | 21.2–342.0 | 1092 $\pm$ 908.5a      | 31.7–2970   |
| Total carbon (%)                   | 1.09 $\pm$ 0.53 b    | 0.63–2.50  | 2.24 $\pm$ 1.97a      | 1.05–9.84  | 0.88 $\pm$ 1.63 b      | 0.10–6.20   |
| Organic carbon (%)                 | 1.06 $\pm$ 0.52 b    | 0.60–2.47  | 2.20 $\pm$ 1.94a      | 1.04–9.71  | 0.31 $\pm$ 0.20 b      | 0–0.61      |
| p-total Pb ( $mg\ kg^{-1}$ )       | 245.7 $\pm$ 312.7c   | 75.6–1390  | 2654 $\pm$ 5709 b     | 68.1–20561 | 19,370 $\pm$ 19905a    | 120.6–59518 |
| p-total Zn ( $mg\ kg^{-1}$ )       | 156.4 $\pm$ 140.5c   | 46.1–602.4 | 1053.9 $\pm$ 1835.1 b | 33.8–6194  | 6134 $\pm$ 5348a       | 146.8–15710 |
| p-total Cd ( $mg\ kg^{-1}$ )       | 0.56 $\pm$ 0.70c     | 0.11–2.54  | 4.03 $\pm$ 6.71 b     | 0.12–24.35 | 26.5 $\pm$ 25.5a       | 0.79–92.3   |
| p-total Cu ( $mg\ kg^{-1}$ )       | 16.3 $\pm$ 7.50 b    | 6.25–38.1  | 90.4 $\pm$ 215.3 b    | 5.10–949.7 | 607.0 $\pm$ 1185a      | 11.7–4409   |
| p-total As ( $mg\ kg^{-1}$ )       | 9.57 $\pm$ 2.87 b    | 4.10–14.03 | 15.48 $\pm$ 17.42 b   | 3.60–84.1  | 40.7 $\pm$ 35.0a       | 3.42–134.9  |
| p-total Ag ( $mg\ kg^{-1}$ )       | 0.64 $\pm$ 1.35 b    | bdl–5.74   | 26.2 $\pm$ 62.7 b     | bdl–221.3  | 81.8 $\pm$ 62.2a       | 0.84–200.0  |
| $CaCl_2$ -extr Pb (%) <sup>*</sup> | 0.02 $\pm$ 0.03a     | 0–0.09     | 0.16 $\pm$ 0.46a      | 0–1.86     | 0.17 $\pm$ 0.24a       | 0–0.91      |
| $CaCl_2$ -extr Zn (%) <sup>*</sup> | 4.09 $\pm$ 3.90 b    | 0.53–13.0  | 3.53 $\pm$ 4.96 b     | 0.10–20.34 | 14.6 $\pm$ 20.5a       | 0–63.2      |
| $CaCl_2$ -extr Cd (%) <sup>*</sup> | 15.1 $\pm$ 11.3 b    | 2.20–40.6  | 11.2 $\pm$ 11.0 b     | 0.37–39.6  | 35.8 $\pm$ 39.2a       | 0.12–100    |
| $CaCl_2$ -extr Cu (%) <sup>*</sup> | 0.19 $\pm$ 0.14 b    | 0.01–0.47  | 0.32 $\pm$ 0.53 ab    | 0–2.12     | 0.74 $\pm$ 1.35a       | 0–4.71      |
| $CaCl_2$ -extr As (%) <sup>*</sup> | 0.08 $\pm$ 0.09a     | 0.02–0.34  | 0.04 $\pm$ 0.03a      | 0.01–0.14  | 0.01 $\pm$ 0.01 b      | 0–0.04      |
| $CaCl_2$ -extr Ag (%) <sup>*</sup> | 0.03 $\pm$ 0.03 b    | 0–0.10     | 0.01 $\pm$ 0.02 b     | bdl–0.06   | 0.21 $\pm$ 0.34a       | bdl–0.96    |

(<sup>\*</sup>) Percentage of  $CaCl_2$ -extractable metals ( $= CaCl_2$ -extractable metal concentration  $\times$  100/Total metal concentration).

Bdl means 'below the detection limit' (Pb = 3  $mg\ kg^{-1}$ , Zn = 9  $mg\ kg^{-1}$ , Cd = 0.2  $mg\ kg^{-1}$ , Cu = 8  $mg\ kg^{-1}$ , As = 0.4  $mg\ kg^{-1}$ , Ag = 1  $mg\ kg^{-1}$ ).

**Table 2**

Correlation matrix between pseudo-total metal concentrations (log-transformed data), pH and electrical conductivity (EC) in the collected samples. (Pearson correlation coefficients, \*\* denotes significance at  $p < 0.01$ ).

| Parameters | pH       | EC      | Pb      | Zn      | Cd      | Cu      | As      | Ag    |
|------------|----------|---------|---------|---------|---------|---------|---------|-------|
| pH         | 1.000    |         |         |         |         |         |         |       |
| EC         | -0.682** | 1.000   |         |         |         |         |         |       |
| Pb         | -0.423** | 0.670** | 1.000   |         |         |         |         |       |
| Zn         | -0.230   | 0.620** | 0.923** | 1.000   |         |         |         |       |
| Cd         | -0.088   | 0.597** | 0.914** | 0.967** | 1.000   |         |         |       |
| Cu         | -0.406** | 0.678** | 0.911** | 0.875** | 0.847** | 1.000   |         |       |
| As         | -0.413** | 0.564** | 0.820** | 0.812** | 0.772** | 0.832** | 1.000   |       |
| Ag         |          | 0.623** | 0.915** | 0.918** | 0.932** | 0.820** | 0.728** | 1.000 |

agrees with our study of San Quintín area in 2006 (Rodríguez et al., 2009), along with other previous studies about Pb–Zn mine sites (Ciarowska et al., 2014; Gabarrón et al., 2018; Khosravi et al., 2018; Liu et al., 2020; Zhou et al., 2020).

The results from the matrix cluster analysis of metal (loid)s are shown in Fig. 2. Regarding mining samples, two main groups of metal (loid)s can be seen: one for the Zn–Cd pair and another which includes the pairs Pb–Ag and Cu–As. The close association between Pb and Ag in the tailings indicates that silver is mainly associated to galena, as well as Cu and As, which would come from micro-inclusions of different mineral phases in galena (Palero-Fernández and Martín-Izard, 2005). The pair Zn–Cd is common in the sphalerite mineral type present in the San Quintín mine and also appears as micro-inclusions in galena (Palero-Fernández and Martín-Izard, 2005). This pattern strongly agrees with that found by Martín-Crespo et al. (2015) for the San Quintín mine but it

is quite different from other reported by Lillo et al. (2014) for the Alcudia Valley mining district; it showed a strong relationship between Cu, Pb and Zn, association that has not been found here. The links between metal (loid)s found for pastureland samples (Fig. 2b) were very similar to those of mine tailings (with the exception of As), providing an additional evidence of the metal (loid) dispersal from tailings in the soils of these areas. On the contrary, the very different association between metal (loid)s found in the arable land samples (Fig. 2a) would reveal a lesser impact in the agricultural plots; since the samples taken corresponded to the first 20 cm of depth, it can be assumed that the work of tilling the soil and the subsequent mixing of soil horizons in those plots have caused the dilution of surface metal (loid) concentrations in some extent.

Although carbon contents of some individual samples reached values near 10% (Table 1), mean values were low for all the soil uses with pastureland samples reaching the highest value (2.24%), which was probably due to the livestock activities in these plots. However, it is important to highlight that while most of the carbon in pastureland and arable land samples was organic, approximately 65% of the carbon in mine tailings samples was inorganic (Table 1). It agrees with the findings of the mineralogical analysis (Table S2), which showed that the major minerals found in the mine tailing samples were quartz, illite and chlorite, but some carbonate minerals such as calcite and dolomite were also detected in significant concentrations (>5%) in some samples (calcite in SQ8 and dolomite in SQ11, SQ21, SQ48 and SQ50).

Fig. 3 shows the maps for the spatial distribution of pseudo-total Pb and Zn concentrations in soils of the San Quintín area. It can be seen that, although the peaks of both metal concentrations are located inside the mining waste areas, the extension of the pollution includes wide areas of pasture and arable lands surrounding the mining site. This is particularly visible in both mining sectors for Zn and in the western sector for Pb. Moreover, it can be seen that the spreading of the pollution from mining areas seems to largely agree with the prevailing wind directions (WSW and ENE, see the wind rose diagram of the area included in Fig. 3) along with the flow direction of runoff (the slope of the terrain decreases mainly to south and southwest in both mining areas, Fig. 1) and surface water streams in the studied area. Therefore, as similar to reported in other agricultural areas surrounding old mining areas (Fernández-Caliani et al., 2009; Gäbler and Schneider, 2000; Gil-Loaiza et al., 2018; Lillo et al., 2014; López et al., 2008) wind-blown dust and the leaching of mine waste and subsequent runoff seem to be the main vectors of metal pollution in San Quintín area. That hypothesis is also reinforced by the results from the matrix cluster analysis shown in Fig. 4. Two main different groups of samples were found, one including all the mine tailings samples (except for SQ17) together with some highly polluted pastureland samples, and other which includes all the arable land samples and most of the pastureland ones. Two of the pastureland samples grouped together with the mining ones, i.e. SQ36 and SQ37, were taken very close to water streams which flows by the borders of the mining areas; another two ones, i.e. SQ32 and SQ33 samples, were located very close to the western sector of the mine in an area that probably belonged to the mining area in the past (Fig. 1). Some other pastureland samples, such as SQ40, SQ46 and SQ41 are also highly

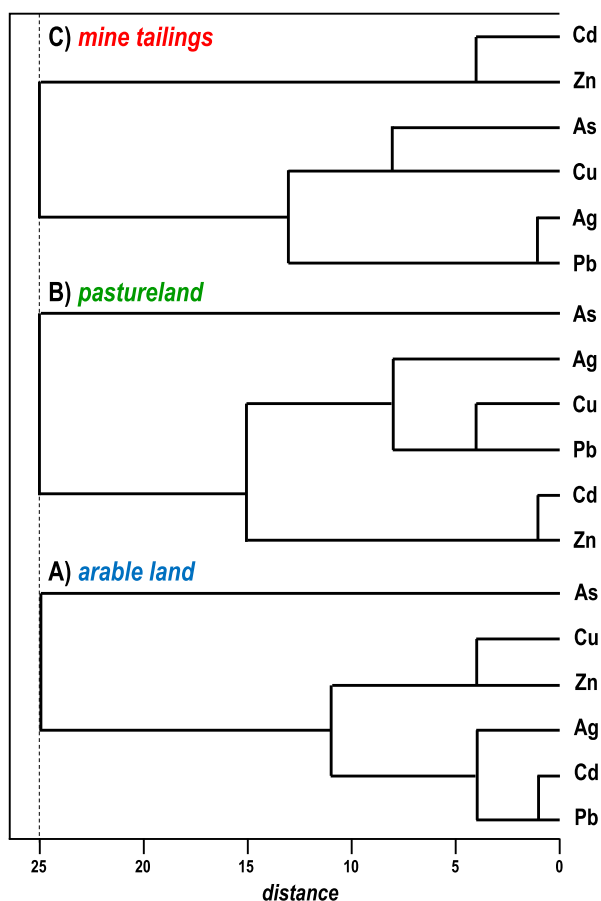


**Fig. 2.** Dendrograms from matrix cluster analysis of metal concentrations by metal (log-transformed data, Ward's method using Euclidean distance squared) for the different types of soil uses: A, arable land samples; B, pastureland samples; C, mine tailings samples.

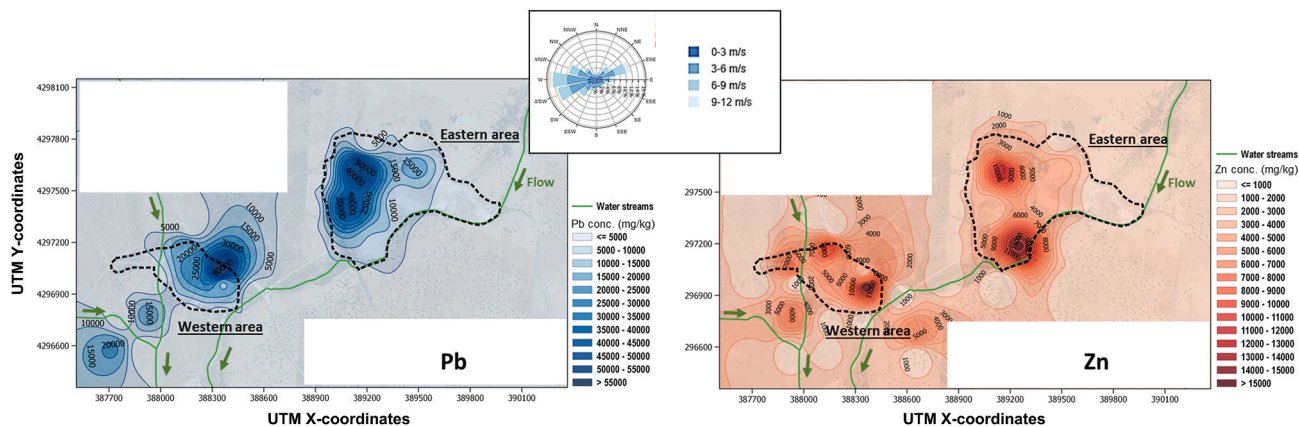


Fig. 3. Interpolation maps of pseudo-total Pb and Zn concentrations in the studied area. Onset of the figure: wind rose for San Quintín mine area, data 1989–2020 (source: ERA-Net Plus NEWA, New European Wind Atlas).

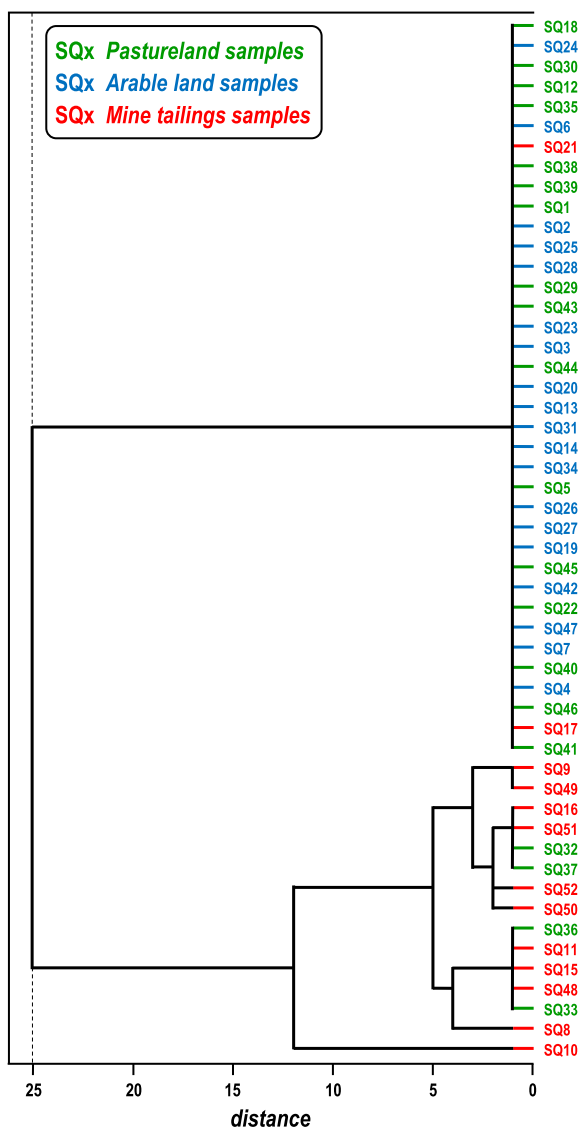


Fig. 4. Dendrograms from matrix cluster analysis of metal concentrations by sample (Ward’s method using Euclidean distance squared), specifying the different types of samples (pastureland in green, arable land in blue and mine tailings in red). (For interpretation of the references to colour in this figure legend, the reader is referred to the Web version of this article.)

polluted and corresponded to areas located south of the western mining sector. However, most of the highest polluted mine samples, i.e. SQ10, SQ8, SQ11, and SQ15, were taken in the eastern sector of the San Quintín mine. Fine-grain mine tailings deposited in this sector, coming from the recovery of sphalerite in the period 1973–1988 (Sánchez-Donoso et al., 2019), would be responsible of the high Zn concentration areas located southwest of it which can be seen in Fig. 2. According to it, lead mineral phases of plumbojarosite ( $PbFe_6(SO_4)_4(OH)_{12}$ ) and/or anglesite ( $PbSO_4$ ), in concentration enough to be detected by X-ray diffraction, were found in several mine samples (Table S2); those minerals are usually found in the tailings from Pb/Zn mines (García-Lorenzo et al., 2019; Oyarzun et al., 2011). Plumbojarosite was also detected in the pastureland sample (SQ37) taken in the bed of one of the water streams located in the studied area; it would come from the precipitation of lead ions transported by runoff from the waste piles. Moreover, since the soluble nature of this secondary lead mineral, it could be easily redissolved and the resulting metal ions subsequently transported by water streams (Lillo et al., 2014).

### 3.2. Medium-term changes in the environmental risk

More interesting than the evaluation of the current pollution in the studied area is to answer to the question about whether the derived environmental risk has changed in the last fourteen years and, if so, in which direction has changed. For this goal, a series of different indices commonly used for the assessment of environmental hazard in soils have been calculated for the pseudo-total metal concentration determined in the samples taken in 2006 and 2020.

In Table 3 are shown the mean values of the different pollution indices for the three soil use types, i.e. arable land, pastureland and mine tailings, and for the two samplings (2006 and 2020). If the comparison of the results from risk assessment is carried out in terms of mean values of the different pollution indices by using analysis of variance (ANOVA), limited conclusions about the changes in the environmental hazard from 2006 to 2020 can be found. Thus, according to Table 3, despite most of the mean values of Igeo, PLI and PER are higher in 2020 as compared to those of 2006, due to the high standard deviations, no statistically significant differences between the two years were found. As expected, the highest values of the pollution indices were obtained for the mine tailings samples which greatly exceeded the threshold values corresponding with the highest risk categories for the indices  $Igeo_{Pb}$ ,  $Igeo_{Zn}$ , PLI and PER in both 2006 and 2020. It highlights, on one hand, the need to do something as soon as possible to prevent tailings from continuing to be a source of pollution in the area and, on the other hand, the opportunity to take advantage of the high metal contents that remain in the waste. Igeo values for Cu corresponded to ‘moderately polluted’ and ‘moderately to highly polluted’ for 2006 and 2020, respectively, while cadmium Igeo

**Table 3**

Risk assessment in San Quintín area in 2006 and 2020: Igeo, Pollution Load Index (PLI) and Potential Ecological Risk index (PER) (Mean values ± STD). Different letters mean significant differences between sample types and years for each index, Duncan's test  $p < 0.05$ .

| Sample type          | Arable land    |                | Pastureland      |                | Mine tailings   |                 |
|----------------------|----------------|----------------|------------------|----------------|-----------------|-----------------|
|                      | 2006           | 2020           | 2006             | 2020           | 2006            | 2020            |
| Igeo Pb <sup>a</sup> | 2.82 ± 1.03a   | 2.63 ± 1.13a   | 3.39 ± 2.20a     | 4.36 ± 2.46a   | 7.53 ± 3.12 b   | 8.26 ± 2.57 b   |
| Igeo Zn              | 0.67 ± 1.30a   | 1.17 ± 1.04 ab | 1.64 ± 1.78 ab   | 2.49 ± 2.35 b  | 5.05 ± 2.56c    | 6.07 ± 1.95c    |
| Igeo Cd              | -1.58 ± 1.07 b | -4.11 ± 1.36a  | -1.17 ± 2.12bc   | -2.43 ± 2.43 b | 0.14 ± 2.07cd   | 1.45 ± 1.75 d   |
| Igeo Cu              | -0.08 ± 0.76a  | -0.14 ± 0.64a  | 0.49 ± 1.15 b    | 0.69 ± 2.00 b  | 2.48 ± 2.20c    | 3.42 ± 2.47c    |
| PLI <sup>b</sup>     | 1.40 ± 1.04a   | 1.78 ± 1.56a   | 4.32 ± 9.04a     | 12.16 ± 21.05a | 50.38 ± 48.36 b | 72.40 ± 68.49 b |
| PER <sup>c</sup>     | 87.1 ± 49.7 ab | 84.9 ± 96.9a   | 321.1 ± 655.5 ab | 843.9 ± 1740 b | 6058 ± 7624c    | 6068 ± 5940c    |

<sup>a</sup> Risk assessment by Igeo: <0, practically unpolluted; 0–1, unpolluted to moderately polluted; 1–2, moderately polluted; 2–3, moderately to strongly polluted; 3–4, strongly polluted; 4–5, strongly to extremely polluted; >5, extremely polluted.

<sup>b</sup> Risk assessment by PLI: ≤1, unpolluted; 1–2, unpolluted to moderately polluted; 2–3, moderately polluted; 3–4, moderately to highly polluted; 4–5, highly polluted; >5, very highly polluted.

<sup>c</sup> Risk assessment by PER: <50, low risk; 50–100, moderate risk; 100–200, considerable risk; >200, very high risk.

values do not indicate hazard from this metal.

A clear proof of the potential of tailings as pollution source is that PLI and PER mean values found for pastureland samples in 2006 and 2020 reached the classification as ‘very high polluted’ and ‘very high risk’, respectively. It is important to remark the high contribution of Pb to the overall risk as evidenced by the high values of the Igeo (corresponding to ‘strongly to extremely polluted’ soils). Similar values of Igeo for Pb and Zn have been recently reported for farmland soils close to historical artisanal zinc smelting areas in China (Zhou et al., 2020). Mean values of the pollution indices corresponding to pastureland samples were in general higher than those of arable land ones, but they were only significantly different for Igeo of Cd and Cu in 2020 and Igeo of Cu in 2006 and for PER in 2020; the reason could be the abovementioned mixing of soil horizons by tilling activities. It is worth noting that the largest increases (but not statistically significant) in the environmental risk indices from 2006 to 2020 were found for the pastureland samples. Thus, Igeo was increased by 29% and 52% for Pb and Zn, respectively, while PLI and PER were 2.8 and 2.6 times higher in 2020 than in 2006.

An additional semiquantitative analysis of the environmental risk can be done by calculating the percentage of samples which are included in the different risk categories derived from the used indices. Thus, Fig. 5 shows that the percentages of the highest risk categories according to Igeo values were increased from 2006 to 2020. For instance, percentages of pastureland samples classified as extremely polluted were increased from 22 to 30% and from 3 to 20% for Pb and Zn, respectively. For mine samples, percentage of extremely polluted samples were also increased up to 28% (for Pb); on the contrary, arable samples were, in general, in a similar risk level for 2006 and 2020 (see Fig. 6).

Similar results can be extracted from the risk categories calculated from PLI and PER. Regarding PER risk assessment, percentages of

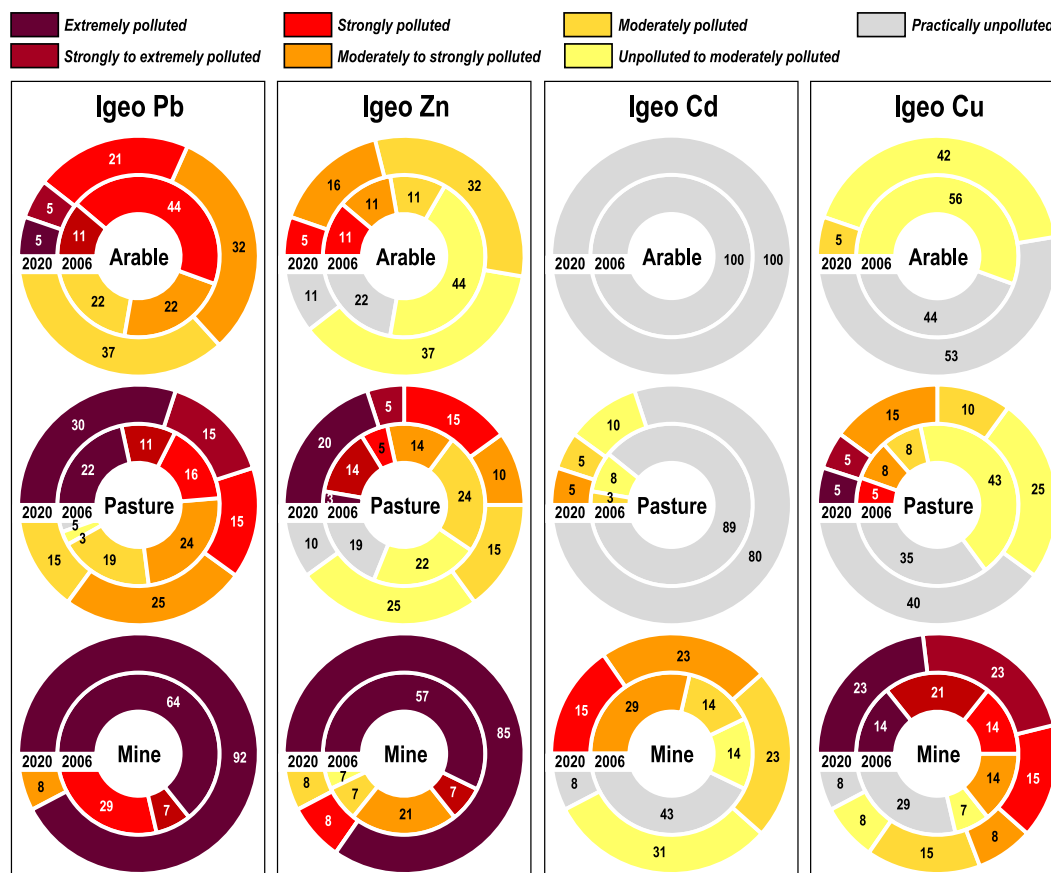


**Fig. 5.** Changes in the environmental risk in San Quintín area in 2006 and 2020 based on the percentage of samples belonging the different risk categories obtained from the geoaccumulation index (Igeo) for Pb, Zn, Cd and Cu.



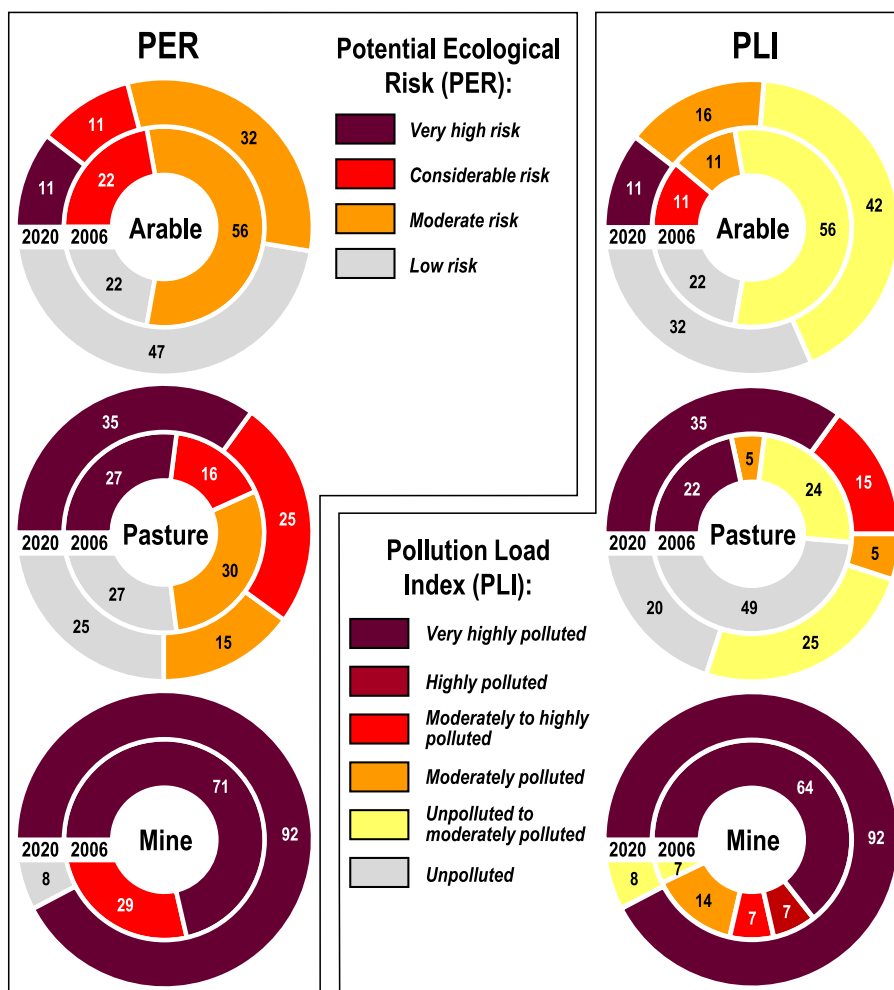


Fig. 6. Changes in the environmental risk in San Quintín area in 2006 and 2020 based on the percentage of samples belonging the different risk categories obtained from the Potential Ecological Risk index (PER) and the Pollution Load Index (PLI).

‘considerable risk’ and ‘very high risk’ pastureland samples were increased in 9 and 8%, respectively, from 2006 to 2020, while the percentage of ‘very high risk’ arable samples increased in 11%; for mine samples, the percentage of samples corresponding with very high risk was increased in 21%. Similar or higher percentage increases in the highest risk category were found using the classification of PLI, i.e. increases of 11, 13 and 28% for arable land, pastureland and mine tailings, respectively, were observed in the category ‘very highly polluted’.

Our results suggest that the environmental risk associated with the mining waste of San Quintín area has clearly increased in some extent in this period, especially in the pastureland areas surrounding the mine. Therefore, it seems clear, in absence of mitigation measures, wind and runoff have been acting as vectors for dispersal of pollution in the surroundings of the San Quintín mine area, potentially compromising the sanitary quality of agricultural and livestock products obtained in adjacent areas, as have been previously reported for some locations of the Alcuía Valley mining area (Reglero et al., 2008; Rodríguez-Estival et al., 2013).

#### 4. Conclusions

Lead and zinc were the most abundant metal (loid)s for all the sample types taken in 2020 in the surrounding of San Quintín mine area, with mean concentrations of Pb being twice or higher than those of Zn. The order of abundance of the rest of analyzed metal (loid)s was Cu > Ag > As > Cd, with average concentrations being at least one order of

magnitude lower than those of Pb and Zn. Metal (loid)s availability (measured as the percentage of CaCl<sub>2</sub>-extractable metals) was only high for Zn and Cd, while it was very low for the rest of metal (loid)s. Concentrations of all analyzed metal (loid)s were in the order mine tailings >> pastureland > arable land. It must be pointed out the high concentration of metal (loid)s found in the pastureland plots adjacent to the mining waste areas with values in at least one order of magnitude (except for Cd) higher than regional background values. The interpolation maps for the pseudo-total concentrations of Pb and Zn seem to support the hypothesis that runoff and wind are the main vectors of dispersion of pollution in the studied area.

The most important conclusions from the environmental risk assessment conducted with data from the samplings of 2006 and 2020 were the following: (i) the environmental hazard found in San Quintín mine area is mainly due to the very high concentration of Pb and Zn, with lesser concern derived from Cu and Cd levels; (ii) excluding the expected high risk in the mining waste areas, the highest environmental risk level, according to the classification based on PLI and PER indices, was detected in the surrounding livestock areas in both years 2006 and 2020; and (iii) environmental risk level in the studied area increased in a high extent from 2006 to 2020, especially in the pastureland areas, with increases up to 17% in the number of soil samples that reached the highest risk classification in 2020 as compared to those taken in 2006. These results demonstrate that environmental risk can actually increase continuously in abandoned mining areas and support the urgent need of taking control measures and/or implementing recovery actions in order



to mitigate the spreading of the pollution and the negative environmental consequences.

### Credit statements

**Luis Rodríguez:** Conceptualization and Methodology, **Jacinto Alonso-Azcárate:** Conceptualization and Methodology and **Francisco J. López-Bellido:** Conceptualization and Methodology. **Hassay L. Medina-Díaz:** Investigation, **Jacinto Alonso-Azcárate:** Investigation and **Beatriz García-Corrochano:** Investigation. **Luis Rodríguez:** Writing – review & editing. **Francisco J. López-Bellido:** Writing – review & editing and **Jacinto Alonso-Azcárate:** Writing – review & editing. **Luis Rodríguez:** Funding acquisition and Project administration and **Francisco J. Fernández-Morales:** Funding acquisition and Project administration.

### Declaration of competing interest

The authors declare that they have no known competing financial interests or personal relationships that could have appeared to influence the work reported in this paper.

### Acknowledgements

This work was supported by the grant PID 2019-107282RB-I00 funded by MCIN/AEI/10.13039/501100011033 (Ministry of Science and Innovation of Spain), and the project SPBLY/19/180501/000254 from European Union (FEDER) and Castilla-La Mancha regional government.

### Appendix A. Supplementary data

Supplementary data to this article can be found online at <https://doi.org/10.1016/j.chemosphere.2021.133129>.

### References

- Aguilar, J., Dorronsoro, C., Fernández, E., Fernández, J., García, I., Martín, F., Simón, M., 2004. Soil pollution by a pyrite mine spill in Spain: evolution in time. *Environ. Pollut.* 132, 395–401. <https://doi.org/10.1016/j.envpol.2004.05.028>.
- Asare, M.O., Afriyie, J.O., 2021. Ancient mining and metallurgy as the origin of Cu, Ag, Pb, Hg, and Zn contamination in soils: a review. *Water, Air, Soil Pollut.* 232, 240. <https://doi.org/10.1007/s11270-021-05166-4>.
- Ballesta, R., Bueno, P., Rubi, J., Giménez, R., 2010. Pedo-geochemical baseline content levels and soil quality reference values of trace elements in soils from the Mediterranean (Castilla La Mancha, Spain). *Open Geosci.* 2 <https://doi.org/10.2478/v10085-010-0028-1>.
- Bănăduc, D., Curtean-Bănăduc, A., Cianfaglione, K., Akeroyd, J.R., Cioca, L.-I., 2021. Proposed environmental risk management elements in a carpathian valley basin, within the roșia montană European historical mining area. *Int. J. Environ. Res. Publ. Health* 18, 4565. <https://doi.org/10.3390/ijerph18094565>.
- Bhattacharya, A., Routh, J., Jacks, G., Bhattacharya, P., Mörth, M., 2006. Environmental assessment of abandoned mine tailings in Adak, Västerbotten district (northern Sweden). *Appl. Geochem.* 21, 1760–1780. <https://doi.org/10.1016/j.apgeochem.2006.06.011>.
- Bravo, S., García-Ordiales, E., García-Navarro, F.J., Amorós, J.Á., Pérez-de-los-Reyes, C., Jiménez-Ballesta, R., Esbrí, J.M., García-Noguero, E.M., Higuera, P., 2019. Geochemical distribution of major and trace elements in agricultural soils of Castilla-La Mancha (central Spain): finding criteria for baselines and delimiting regional anomalies. *Environ. Sci. Pollut. Res.* 26, 3100–3114. <https://doi.org/10.1007/s11356-017-0010-6>.
- Chen, H., Chen, Zhibiao, Chen, Zhiqiang, Ou, X., Chen, J., 2020. Calculation of toxicity coefficient of potential ecological risk assessment of rare earth elements. *Bull. Environ. Contam. Toxicol.* 104, 582–587. <https://doi.org/10.1007/s00128-020-02840-x>.
- Chen, H., Teng, Y., Lu, S., Wang, Y., Wang, J., 2015. Contamination features and health risk of soil heavy metals in China. *Sci. Total Environ.* 512–513, 143–153. <https://doi.org/10.1016/j.scitotenv.2015.01.025>.
- Chopin, E.I.B., Black, S., Hodson, M.E., Coleman, M.L., Alloway, B.J., 2003. A preliminary investigation into mining and smelting impacts on trace element concentrations in the soils and vegetation around Tharsis, SW Spain. *Mineral. Mag.* 67, 279–288. <https://doi.org/10.1180/0026461036720099>.
- Ciarkowska, K., Solec-Podwika, K., Wiecezorek, J., 2014. Enzyme activity as an indicator of soil-rehabilitation processes at a zinc and lead ore mining and processing area. *J. Environ. Manag.* 132, 250–256. <https://doi.org/10.1016/j.jenvman.2013.10.022>.
- Concas, A., Ardu, C., Cristini, A., Zuddas, P., Cao, G., 2006. Mobility of heavy metals from tailings to stream waters in a mining activity contaminated site. *Chemosphere* 63, 244–253. <https://doi.org/10.1016/j.chemosphere.2005.08.024>.
- Djebbi, C., Chaabani, F., Font, O., Queralt, I., Querol, X., 2017. Atmospheric dust deposition on soils around an abandoned fluorite mine (Hammam Zriba, NE Tunisia). *Environ. Res.* 158, 153–166. <https://doi.org/10.1016/j.envres.2017.05.032>.
- Doabi, S.A., Karami, M., Afyuni, M., Yeganeh, M., 2018. Pollution and health risk assessment of heavy metals in agricultural soil, atmospheric dust and major food crops in Kermanshah province, Iran. *Ecotoxicol. Environ. Saf.* 163, 153–164. <https://doi.org/10.1016/j.ecoenv.2018.07.057>.
- Fernández-Caliani, J.C., Barba-Brioso, C., González, I., Galán, E., 2009. Heavy metal pollution in soils around the abandoned mine sites of the Iberian pyrite belt (Southwest Spain). *Water Air Soil Pollut.* 200, 211–226. <https://doi.org/10.1007/s11270-008-9905-7>.
- Gabarrón, M., Faz, A., Martínez-Martínez, S., Acosta, J.A., 2018. Change in metals and arsenic distribution in soil and their bioavailability beside old tailing ponds. *J. Environ. Manag.* 212, 292–300. <https://doi.org/10.1016/j.jenvman.2018.02.010>.
- Gäbler, H.E., Schneider, J., 2000. Assessment of heavy-metal contamination of floodplain soils due to mining and mineral processing in the Harz Mountains, Germany. *Environ. Geol.* 39, 774–782. <https://doi.org/10.1007/s002540050493>.
- García-Carmona, M., García-Robles, H., Turpin Torrano, C., Fernández Ondoño, E., Lorite Moreno, J., Sierra Aragón, M., Martín Peinado, F.J., 2019. Residual pollution and vegetation distribution in amended soils 20 years after a pyrite mine tailings spill (Aznalcóllar, Spain). *Sci. Total Environ.* 650, 933–940. <https://doi.org/10.1016/j.scitotenv.2018.09.092>.
- García-Lorenzo, M.L., Crespo-Feo, E., Esbrí, J.M., Higuera, P., Grau, P., Crespo, I., Sánchez-Donoso, R., 2019. Assessment of potentially toxic elements in technosols by tailings derived from Pb–Zn–Ag mining activities at san Quintín (Ciudad real, Spain): some insights into the importance of integral studies to evaluate metal contamination pollution hazards. *Minerals* 9, 346. <https://doi.org/10.3390/min9060346>.
- Gil-Loaiza, J., Field, J.P., White, S.A., Csavina, J., Felix, O., Betterton, E.A., Sáez, A.E., Maier, R.M., 2018. Phytoremediation reduces dust emissions from metal(loids)-contaminated mine tailings. *Environ. Sci. Technol.* 52, 5851–5858. <https://doi.org/10.1021/acs.est.7b05730>.
- Gitari, M.W., Akinyemi, S.A., Ramugondo, L., Matidza, M., Mhlongo, S.E., 2018. Geochemical fractionation of metals and metalloids in tailings and appraisal of environmental pollution in the abandoned Musina Copper Mine, South Africa. *Environ. Geochem. Health* 40, 2421–2439. <https://doi.org/10.1007/s10653-018-0109-9>.
- Hakanson, L., 1980. An ecological risk index for aquatic pollution control. a sedimentological approach. *Water Res.* 14, 975–1001. [https://doi.org/10.1016/0043-1354\(80\)90143-8](https://doi.org/10.1016/0043-1354(80)90143-8).
- Islam, S., Ahmed, K., Habibullah-Al-Mamun, Masunaga, S., 2015. Potential ecological risk of hazardous elements in different land-use urban soils of Bangladesh. *Sci. Total Environ.* 512–513, 94–102. <https://doi.org/10.1016/j.scitotenv.2014.12.100>.
- Khosravi, V., Doulati Ardejani, F., Yousefi, S., Aryafar, A., 2018. Monitoring soil lead and zinc contents via combination of spectroscopy with extreme learning machine and other data mining methods. *Geoderma* 318, 29–41. <https://doi.org/10.1016/j.geoderma.2017.12.025>.
- Kicińska, A., 2020. Lead and zinc in soils around a zinc-works-presence, mobility and environmental risk. *J. Ecol. Eng.* 21 <https://doi.org/10.12911/22998993/119815>.
- Kicińska, A., 2019. Environmental risk related to presence and mobility of As, Cd and Tl in soils in the vicinity of a metallurgical plant – long-term observations. *Chemosphere* 236. <https://doi.org/10.1016/j.chemosphere.2019.07.039>.
- Lillo, J., Oyarzun, R., Esbrí, J.M., García-Lorenzo, M.L., Higuera, P., 2014. Pb–Zn–Cd–As pollution in soils affected by mining activities in central and southern Spain: a scattered legacy posing potential environmental and health concerns. In: *Handbook of Environmental Chemistry*, pp. 175–205. <https://doi.org/10.1007/978-94-007-278-1>.
- Liu, J., Yin, M., Luo, X., Xiao, T., Wu, Z., Li, N., Wang, J., Zhang, W., Lippold, H., Belshaw, N.S., Feng, Y., Chen, Y., 2019. The mobility of thallium in sediments and source apportionment by lead isotopes. *Chemosphere* 219, 864–874. <https://doi.org/10.1016/j.chemosphere.2018.12.041>.
- Liu, K., Li, C., Tang, S., Shang, G., Yu, F., Li, Y., 2020. Heavy metal concentration, potential ecological risk assessment and enzyme activity in soils affected by a lead-zinc tailing spill in Guangxi, China. *Chemosphere* 251, 126415. <https://doi.org/10.1016/j.chemosphere.2020.126415>.
- López, M., González, I., Romero, A., 2008. Trace elements contamination of agricultural soils affected by sulphide exploitation (Iberian Pyrite Belt, SW Spain). *Environ. Geol.* 54, 805–818. <https://doi.org/10.1007/s00254-007-0864-x>.
- Luo, W., Lu, Y., Giesy, J.P., Wang, T., Shi, Y., Wang, G., Xing, Y., 2007. Effects of land use on concentrations of metals in surface soils and ecological risk around Guanting Reservoir, China. *Environ. Geochem. Health* 29, 459–471. <https://doi.org/10.1007/s10653-007-9115-z>.
- Martín-Crespo, T., Gómez-Ortiz, D., Martín-Velázquez, S., Esbrí, J.M., de Ignacio-San José, C., Sánchez-García, M.J., Montoya-Montes, I., Martín-González, F., 2015. Abandoned mine tailings in cultural itineraries: don Quixote Route (Spain). *Eng. Geol.* 197, 82–93. <https://doi.org/10.1016/j.enggeo.2015.08.008>.
- Muller, G., 1969. Index of geo-accumulation in sediments of the rhine river. *Geojournal* 2, 108–118.
- Novozamsky, I., Lexmond, T.M., Houba, V.J.G., 1993. A single extraction procedure of soil for evaluation of uptake of some heavy metals by plants. *Int. J. Environ. Anal. Chem.* 51 <https://doi.org/10.1080/03067319308027610>.
- Oyarzun, R., Lillo, J., López-García, J.A., Esbrí, J.M., Cubas, P., Llanos, W., Higuera, P., 2011. The Mazarrón Pb–(Ag)–Zn mining district (SE Spain) as a source of heavy

- metal contamination in a semiarid realm: geochemical data from mine wastes, soils, and stream sediments. *J. Geochem. Explor.* 109, 113–124. <https://doi.org/10.1016/j.jgexplo.2010.04.009>.
- Palero-Fernández, F.J., Martín-Izard, A., 2005. Trace element contents in galena and sphalerite from ore deposits of the Alcuía Valley mineral field (Eastern Sierra Morena, Spain). *J. Geochem. Explor.* 86, 1–25. <https://doi.org/10.1016/j.jgexplo.2005.03.001>.
- Qing, X., Yutong, Z., Shenggao, L., 2015. Assessment of heavy metal pollution and human health risk in urban soils of steel industrial city (Anshan), Liaoning, Northeast China. *Ecotoxicol. Environ. Saf.* 120, 377–385. <https://doi.org/10.1016/j.ecoenv.2015.06.019>.
- Reglero, M.M., Monsalve-González, L., Taggart, M.A., Mateo, R., 2008. Transfer of metals to plants and red deer in an old lead mining area in Spain. *Sci. Total Environ.* 406, 287–297. <https://doi.org/10.1016/j.scitotenv.2008.06.001>.
- Rehman, I. ur, Ishaq, M., Ali, L., Khan, S., Ahmad, I., Din, I.U., Ullah, H., 2018. Enrichment, spatial distribution of potential ecological and human health risk assessment via toxic metals in soil and surface water ingestion in the vicinity of Sewakht mines, district Chitral, Northern Pakistan. *Ecotoxicol. Environ. Saf.* 154, 127–136. <https://doi.org/10.1016/j.ecoenv.2018.02.033>.
- Rodríguez-Estival, J., Álvarez-Lloret, P., Rodríguez-Navarro, A.B., Mateo, R., 2013. Chronic effects of lead (Pb) on bone properties in red deer and wild boar: relationship with vitamins A and D3. *Environ. Pollut.* 174, 142–149. <https://doi.org/10.1016/j.envpol.2012.11.019>.
- Rodríguez, L., Ruiz, E., Alonso-Azcárate, J., Rincón, J., 2009. Heavy metal distribution and chemical speciation in tailings and soils around a Pb–Zn mine in Spain. *J. Environ. Manag.* 90, 1106–1116. <https://doi.org/10.1016/j.jenvman.2008.04.007>.
- Sánchez-Donoso, R., Martín-Duque, J.F., Crespo, E., Higuera, P.L., 2019. Tailings geomorphology of the San Quintín mining site (Spain): landform catalogue, aeolian erosion and environmental implications. *Environ. Earth Sci.* 78, 166. <https://doi.org/10.1007/s12665-019-8148-9>.
- Tian, H., Fang, L., Duan, C., Wang, Y., Wu, H., 2018. Dominant factor affecting Pb speciation and the leaching risk among land-use types around Pb–Zn mine. *Geoderma* 326, 123–132. <https://doi.org/10.1016/j.geoderma.2018.04.016>.
- Tomlinson, D.L., Wilson, J.G., Harris, C.R., Jeffrey, D.W., 1980. Problems in the assessment of heavy-metal levels in estuaries and the formation of a pollution index. *Helgol. Meeresunters.* 33, 566–575. <https://doi.org/10.1007/BF02414780>.
- Zhou, Yuting, Wang, L., Xiao, T., Chen, Y., Beiyuan, J., She, J., Zhou, Yuchen, Yin, M., Liu, J., Liu, Y., Wang, Y., Wang, J., 2020. Legacy of multiple heavy metal(loid)s contamination and ecological risks in farmland soils from a historical artisanal zinc smelting area. *Sci. Total Environ.* 720, 137541. <https://doi.org/10.1016/j.scitotenv.2020.137541>.